

# Capturing heterotachy through multi-gamma site models

Remco Bouckaert<sup>1,2</sup>, Peter Lockhart<sup>3</sup>

`remco@cs.auckland.ac.nz` `P.J.Lockhart@massey.ac.nz`

1: University of Auckland, 2: Max Planck Institute, 3: Massey University

April 15, 2015

## Abstract

Most methods for performing a phylogenetic analysis based on sequence alignments of gene data assume that the mechanism of evolution is constant through time. It is recognised that some sites do evolve somewhat faster than others, and this can be captured using a (gamma) rate heterogeneity model. Further, some species have shorter replication times than others, and this results in faster rates of substitution in some lineages. This feature of lineage specific rate variation can be captured to some extent, by using relaxed clock models. However, it is also clear that there are additional poorly characterised features of sequence data that can sometimes lead to extreme differences in lineage specific rates. This variation is poorly captured by constant time reversible substitution models. The significance of extreme lineage specific rate differences is that they lead both to errors in reconstructing evolutionary relationships as well as biased estimates for the age of ancestral nodes. We propose a new model that allows gamma rate heterogeneity to change on branches, thus offering a more realistic model of sequence evolution. It adds negligible computational cost to likelihood calculations. We illustrate its effectiveness with an example of green algae and land-plants. For many real world data sets, we find a much better fit with multi-gamma sites models as well as substantial differences in ancestral node date estimates.

## 1 Introduction

Systematic error is one of the major concerns of phylogenetic reconstruction, as it can mislead tree building. Heterotachy [22, 24] – the inference of lineage specific rate variation – is one problem and potential cause of systematic error. Heterotachy is present in many data sets [22]. Different underlying processes of evolution can explain heterotachy [20], one of these being that changes in intermolecular interactions over time can affect which and how many sites are free to vary [16, 15]. To some extent, the processes of nucleotide and amino acid substitution can be accommodated by covarion and gamma distributed

substitution models [12, 20, 23, 28, 29]. To maintain time reversibility, these models assume that the number of sites assigned to a particular evolutionary rate class sequence remains constant through time [30]. However, this might not be a realistic biological assumption. Numerous observations suggest that the proportion of variable sites in homologues changes over larger evolutionary distances [15, 19, 21] (but see also [33] regarding sufficiency). A consequence of this form of non-stationarity, when modelling sequence evolution using a discrete gamma distribution, is that the alpha shape parameter, which describes the proportion of sites assigned to a particular rate class, will change across the underlying tree [30].

For the gamma rate heterogeneity model to be consistent, combining two samples should result in similar shape parameter estimates. However, it is well known that different sampling strategies result can in different estimates of the shape parameter [28]. This suggests that the rate heterogeneity is not constant, but changes throughout the tree, which justifies investigating models that allow such shape variation.

Here we investigate heterotachy and its impact on topology and divergence time estimates in the green plant evolutionary lineage. This is one of the oldest and most diverse branches of the tree of life. Researchers reconstructing evolutionary relationships with green plants face difficulties in phylogenetic reconstruction similar to those being faced elsewhere by others [24]. The challenge is worthwhile, as overcoming the problems will lead to insight into unresolved questions such as: What was the nature of the earliest angiosperms and land plants? How many times was land colonised from the water by “green algae”? Where did the key adaptive features for life on land come from? How many times has multicellularity arisen in the green plants? Did multicellularity ever reverse? How many times did alternation of generations and diploid-dominant life-cycles arise? While justifiable emphasis has been placed on the importance of taxon sampling, increasing attention is now being focussed on the problem of data-model fit [6]. Here, we examine the potential of multi-gamma and relaxed-gamma site models to improve data-model fit and in so doing improve phylogenetic inference. We describe our findings and implement these new models in the open source software BEAST and thus introduced a practical and user friendly way to model shape parameter variation throughout the tree.

## 2 Methods

First, we revisit the classic gamma rate heterogeneity model, before describing the multi-gamma model and the relaxed-gamma model.

### 2.1 Gamma site model (with invariant sites)

The likelihood of the data in an alignment  $D$  for tips of a tree  $g$  is:

$$L(g) = \Pr\{D|g, \Omega\},$$

where  $\Omega = \{Q, \mu\}$  includes parameters  $Q$  of the substitution model and the overall rate  $\mu$ . Consider edges  $\langle i, j \rangle \in R$  of tree  $g = \{R, \mathbf{t}\}$ , and node heights  $t_i$  and  $t_j$ , and let the entry  $s_{i,k}$  be a nucleotide base at site  $k$  of the sequence at node  $i$ . As usual, we assume the sites in the alignment are independent, and the alignment represents data at the tips, but not for internal nodes. Then we sum over all possible ancestral sequences  $D_Y$  for assignments of internal node to get Felsenstein's tree likelihood [11] which can be written as

$$\Pr\{D|g, \Omega\} = \sum_{D_Y \in \mathcal{D}} \prod_{\langle i, j \rangle \in R} \prod_{k=1}^L \left[ e^{Q\mu(t_i - t_j)} \right]_{s_{i,k}, s_{j,k}}.$$

This likelihood assumes constant rates over all sites, which is not realistic in many situations. Yang et al. [34] introduced a model that assumes site rates are distributed according to a gamma distribution  $\Gamma(\alpha, \frac{1}{\alpha})$  with mean one, leaving one shape parameter  $\alpha$ . The likelihood can be written as

$$\Pr\{D|g, \Omega\} = \prod_{k=1}^L \int_{r=0}^{\infty} \Gamma(r|\alpha, \frac{1}{\alpha}) \left( \sum_{D_Y \in \mathcal{D}} \prod_{\langle i, j \rangle \in R} \left[ e^{Q\mu r(t_i - t_j)} \right]_{s_{i,k}, s_{j,k}} \right) dr. \quad (1)$$

which can be efficiently calculated using Felsenstein's peeling algorithm [11]. Computationally, it is convenient to approximate the integral by a sum over  $K$  categories with rates  $r_c(\alpha)$  for category  $c$  representing the mean of the  $k$ th quantile of the gamma distribution with mean 1 and shape parameter  $\alpha$ . The likelihood can be calculated as a mixture of likelihoods with rates  $r_c(\alpha)$  as

$$\Pr\{D|g, \Omega\} = \prod_{k=1}^L \sum_{c=1}^K \frac{1}{K} \left( \sum_{D_Y \in \mathcal{D}} \prod_{\langle i, j \rangle \in R} \left[ e^{Q\mu r_c(\alpha)(t_i - t_j)} \right]_{s_{i,k}, s_{j,k}} \right). \quad (2)$$

Often, there are many constant sites, and a rate of zero would fit best for these sites. Adding another category  $r_1 = 0$  with invariant sites [14, 32] for a proportion  $p_1$  of the mixture, and using the remainder for the gamma rate model with  $K$  categories, the likelihood becomes

$$\Pr\{D|g, \Omega\} = \prod_{k=1}^L \sum_{c=1}^{K+1} p_c \left( \sum_{D_Y \in \mathcal{D}} \prod_{\langle i, j \rangle \in R} \left[ e^{Q\mu r_c(\alpha)(t_i - t_j)} \right]_{s_{i,k}, s_{j,k}} \right). \quad (3)$$

where  $p_c = \frac{1-p_1}{K}$  for  $c > 1$  and  $r_c(\alpha)$  the mean of the  $c - 1$ th quantile of the gamma distribution for  $c > 1$ .

## 2.2 Multi-gamma site model

In the gamma rate heterogeneity model, the shape parameter  $\alpha$  is assumed to be constant throughout the tree. In the *multi-gamma model* we assume that for each branch and in node  $i$  in the tree, we have an individual shape parameter

$\alpha_i$  governing the heterogeneity of the rates. Practically, this means replacing the rate  $r_c(\alpha)$  in Equation (1) with rate  $r_c(\alpha_i)$ .

To distinguish this model from Yang’s model, we call the latter the *single-gamma mode* in the remainder of this paper. An obvious disadvantage is that in a tree with  $n$  branches, we need to estimate  $n$  parameters for multi-gamma model while only a single parameter needs to be estimated for the single-gamma model.

Our experience it that this is achievable in practice if there is sufficient heterotachy in the data, and it looks like a good option for maximum likelihood implementations. However, care must be taken with binary rooted trees, since the shape parameters for branches to the root appears to be unidentifiable in practice.

### 2.3 Relaxed-gamma site model

Instead of estimating the individual shape parameters, we can assume they are distributed according to a density  $p(\alpha|\theta)$  shared by all shape parameters and integrate them out.  $\Pr\{D|g, \Omega\}$  becomes

$$= \int_{\alpha_q} \cdots \int_{\alpha_n} \prod_{k=1}^L \sum_{c=1}^K \frac{1}{K} \left( \sum_{D_Y \in \mathcal{D}} \prod_{\langle i,j \rangle \in R} \left[ e^{Q\mu r_c(\alpha)(t_i - t_j)} \right]_{s_{i,k}, s_{j,k}} \right) p(\alpha_1|\theta) \cdots p(\alpha_n|\theta) d\alpha_1 \cdots d\alpha_n. \quad (4)$$

We call this model the *relaxed-gamma model* to distinguish it from the single and multi-gamma models. Note that the number of parameters in this model is just the cardinality of  $\theta$ . If  $p(\alpha|\theta)$  is a log-normal or gamma distribution, there are just two parameters, which is just a single parameter more than the single-gamma model.

Unfortunately, calculating Equation (4) directly is not feasible, so we use MCMC in a Bayesian setting to approximate these integrals in a similar fashion as done for the uncorrelated relaxed model [8]. The density  $p(\alpha)$  can be discretised into a number of quantiles. Earlier findings [18, 25] suggests that setting the number of quantiles equal to the number of branches is appropriate that number is larger than 100. For each quantile  $q$ , we calculate the mean value  $m_q$  and for each branch  $i$ , and we maintain an index  $a_i$  of a quantile for that branch. We use the following proposals

- a proposal, that randomly selects a branch and randomly selects a new value for the index  $a_i$  inside a window of its old value,
- a proposal that randomly selects a branch and randomly selects a new value for the index  $a_i$  in its range,
- a proposal that randomly selects two branches and swaps their indices,
- a proposal to scale the parameters of the density  $p(\alpha|\theta)$  for each of the parameters in  $\theta$ .

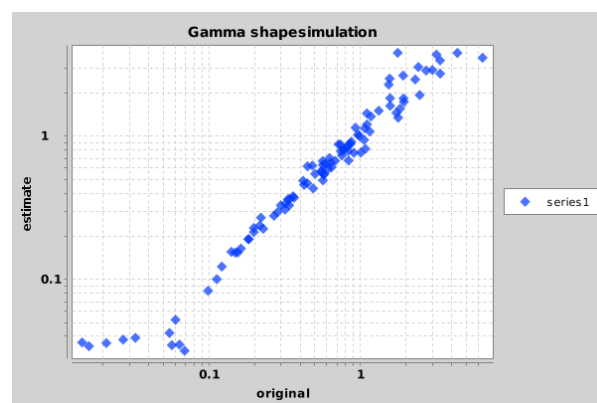


Figure 1: Simulated (horizontal axis) and estimated (vertical axis) values of gamma shapes when simulating with single gamma. Both axis are log-scale.

## 2.4 Miscellaneous

Similar to the single gamma model with a category for invariant sites, the multi-gamma and relaxed gamma models can be extended to include invariant sites by generalising Equation (3) in a similar way we generalised Equation (2) by adding a category with rate zero for all branches.

*Remark:* We did not make any assumptions about the tree, so the theory applies to unrooted, rooted and rooted time trees [8], binary trees as well as polytopies and sampled ancestor trees [13].

Note that the computation complexity of the tree-likelihood – Equation (1) – adapted for the multi-gamma or relaxed gamma model using the Felstein’s peeling algorithm does not change, so no extra computational cost is incurred in calculating the likelihood. Of course, since the parameter space is larger for these models, longer computation is required to estimate these extra parameters.

## 3 Results

In this section, we show the effectiveness of the model using a simulation study and using randomly selected alignments from TreeBase [26], alignments from the PartitionFinder dataset repository <https://github.com/roblanf/PartitionedAlignments> and a case study concerning the evolutionary relationships of green plants and algae.

### 3.1 Simulation study

First, we establish how reliably the shape parameter of the single-gamma model can be estimated. The shape parameter  $\alpha$  was sampled from the exponential

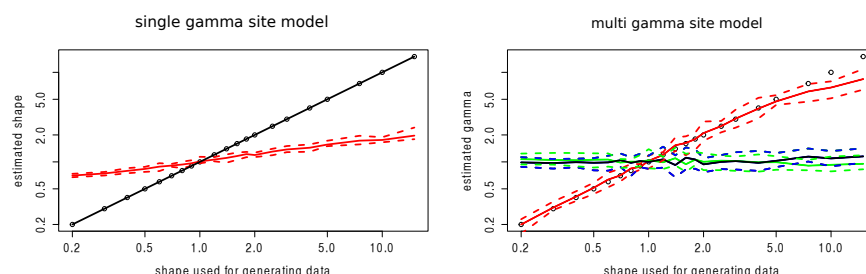


Figure 2: Simulated and estimated values of gamma shapes when varying a single gamma and leave the remaining at 1. Both axis are log-scale.

distribution with mean 1, which is commonly used as prior for the shape parameter. Sequences of 10,000 sites were simulated under the HKY model on a tree with 3 taxa  $((A, B), C)$  and a single-gamma model with four categories. The simulation study was performed using BEASTShell [2]. Then, an analysis under the same model was done in BEAST where  $\alpha$  was estimated. Figure 1 shows the sampled  $\alpha$  on the x-axis and estimated  $\alpha$  on the y-axis. It shows that  $\alpha$  can be estimated correctly over a large range, though it underestimates the alpha value for very large values and overestimates the alpha value for very small values. This is to be expected, since these extreme values, though rare, do not leave a large trace in the data, so the prior pulls the estimate towards the mean of 1.0. Note that smaller  $\alpha$  values are estimated with lower error than higher  $\alpha$  values.

We repeated the experiment, but instead of keeping  $\alpha$  constant throughout the tree, only the  $\alpha$  for a single branch in taxon  $A$  was varied. The left of Figure 2 shows what happens when we estimated  $\alpha$  using the single-gamma model; it appears that the estimated  $\alpha$  is the mean of the simulated  $\alpha$  values, when branch lengths are taken into account. The  $\alpha$  value that was varied does not dominate the estimate. The right of Figure 2 shows  $\alpha$  values for individual branches. There is some increase in the uncertainty of the estimates, but simulated values remain in the 95%HPD of estimated values, again with the exception of extreme  $\alpha$  values. In conclusion, our observations show that under the simulated conditions the multi-gamma model can recover shape parameters.

### 3.2 Nucleotide alignments from TreeBase

To get an impression of how the multi-gamma model performs on empirical data, we randomly selected 50 nucleotide alignments of various sizes from TreeBase [26]. Appendix A lists the details of the alignments. The analysis uses a HKY substitution model [17], the uncorrelated relaxed clock model with log normal distribution [9] and Yule tree prior [35]. The model was run both with single gamma and a category for invariant sites, and results compared with the multi-

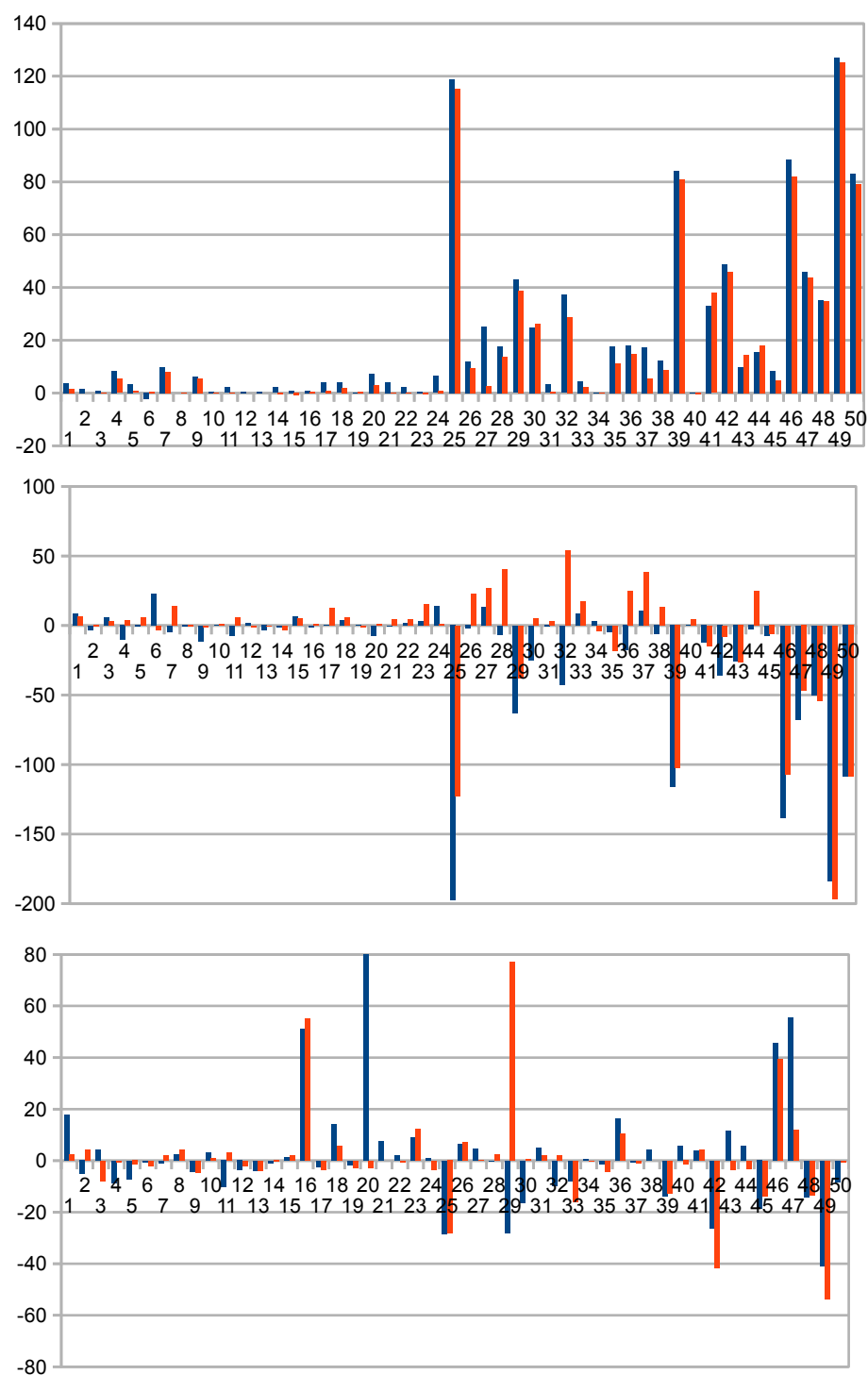


Figure 3: Results for 50 TreeBase alignments ordered in alignment size from small to big comparing single gamma, with multi-gamma models (in blue) and relaxed gamma models (in red). Difference in log likelihoods at the top (higher favours multi-gamma models) and difference of AICM in the middle (lower favours multi gamma models). The bottom shows percentage change in root height estimates.

gamma and relaxed gamma model, both with a category for invariant sites. The analyses were run till convergence, judging from effective sample sizes of at least 200.

Figure 3 shows results for the 50 datasets in order of alignment size, which is the number of nucleotides contained in the alignment, that is, the number of taxa times the length of the alignment. The top shows differences in likelihood estimates and AICM [1] scores for these analyses. It appears that for smaller alignments, there is not much benefit of using the multi-gamma model. However, it does not cause much damage either. For larger alignments, there can be significant improvement of the fit. Given these data sets were randomly selected, we expect this to be true for many data sets in general.

The bottom of Figure 3 shows there are sometimes dramatic differences in divergence time estimates. This observation highlights the concern for the impact that model misspecification can have on molecular dating.

This conclusion is supported by similar analyses of the datasets from the partition finder repository (see Appendix D). Comparing results for single and relaxed gamma site models that assume a proportion of invariable sites, we find that for those datasets that converged (not all of them did, since some datasets were too large to converge over the period of analysis) relaxed gamma site models in general fit better for any substantial dataset, judging from AICM estimates. Further, time estimates can differ considerably between models.

### 3.3 Dating the origin of green plants and algae

We collected a set of 34 *atpB* and *rpoC1* chloroplast genes from Genbank (see Appendix B for accession numbers), aligned their inferred protein sequences using MUSCLE [10] in MEGA [31] and then converted the protein sequences back to nucleotides. This produced data matrices for *atpB* with 1401 sites (749 patterns) and for *rpoC1* with 1359 sites (1097 patterns). Furthermore, we constrained the tree to the topology shown in Figure 4 and we have two calibrations one on the stem leading to angiosperms following divergence from conifers and one on the stem leading to ferns subsequent to their divergence from seed plants [27] (Figure 4).

Data was analysed in BEAST [5] by assuming a separate partition for each codon position. A reversible-jump based substitution model [3] was used and GTR was found to be preferred in all cases, with the exception of partition 3 of the *atpB* dataset, for which the EVS model was preferred. A discrete four category gamma distribution model that also assumed invariable sites, was found to fit the data much better than a model that assumed no positional rate heterogeneity or a model that assumed a single rate class plus invariable sites. We used an uncorrelated relaxed clock (log normal) model [9] for branches, and estimated a coefficient of variation of around 0.7 for both genes. This result indicates that that the strict clock can be rejected. A Yule process was assumed for the tree prior. The main issue when using a single-gamma site model is that root height estimates differ considerably, with mean estimates leaving a gap of over 100M year. Also, the topology in the part of the tree that is not







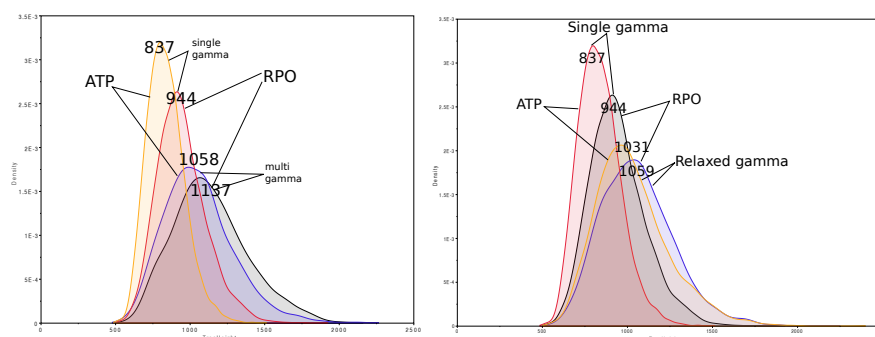


Figure 7: Root height estimates under the various models.

rates are higher for multi-gamma and relaxed-gamma models (mean rate  $6.86\text{E-}10$  and  $1.03\text{E-}9$  substitutions per site per year for single gamma and  $9.17\text{E-}10$  and  $1.04\text{E-}9$  s/s/y for relaxed-gamma model for APT and rpoC1 respectively). The higher clock rate is consistent with a better fit, but one would expect a lower root to accommodate the mutations in the data, but the models also infer a higher root date instead of a lower one. This suggests that for this data the multi/relaxed gamma model accommodate more mutations. An alternative interpretation of our results is that the single-gamma model underestimates the amount of mutation.

The analysis was repeated with *atpB* and *rpoC1* concatenated into a single alignment, which seems reasonable given both are from the chloroplast genome, hence must share a common history. Essentially, all results can be interpreted as the average of the results for the individual *atpB* and *rpoC1* analyses. The fit for multi/relaxed-gamma is still much better than for single gamma, the root estimate higher, and in between that of *atpB* and *rpoC1* individually, and topology estimate is partly compatible with the *atpB* topology and partly with the *rpoC1* topology.

## 4 Discussion

We introduced a Bayesian framework for allowing shape parameters governing rate heterogeneity to vary across branches. The method allows us to get consistent time estimates for different chloroplast genes for green plants, while without the multi-gamma rate model we get substantially different estimates. This suggests that the heterotachy suspected for this data can be captured effectively through multi-gamma site models. Furthermore, for many datasets, the method gives a much better fit as well as different time estimates.

The method is implemented in the MGSM (multi-gamma site model) package for BEAST [5]. It is open source and freely available under LGPL license from <https://github.com/BEAST2-Dev/MGSM/>, and offers GUI support

through BEAUti for setting up an analysis (see <https://github.com/BEAST2-Dev/MGSM/wiki>).

It did not escape our attention that the techniques for handling branch related parameters as in the multi-gamma and relaxed gamma models could be used for other features of substitution models over branches. Possible directions for generalising multi-gamma site models include site models with a limited number of gamma shapes, in a similar fashion as clock models such as the random local clock [7] can have a limited number of branch rates in between 1 and the total number of branches.

## Acknowledgements

This work was assisted by stimulating discussions with Chris Simon and Dave Marshall as well as comments at the New Zealand Phylogenomics 2015 meeting. This work was funded by a Rutherford fellowship (<http://www.royalsociety.org.nz/programmes/funds/rutherford-discovery/>) from the Royal Society of New Zealand awarded to Prof. Alexei Drummond.

## References

- [1] G. Baele, P. Lemey, T. Bedford, A. Rambaut, M. A. Suchard, and A. V. Alekseyenko. Improving the accuracy of demographic and molecular clock model comparison while accommodating phylogenetic uncertainty. *Mol. Biol. Evol.*, 29(9):2157–2167, 2012.
- [2] Remco R. Bouckaert. Beastshell – scripting for bayesian hierarchical clustering. *Submitted*, 2015.
- [3] Remco R. Bouckaert, Mónica Alvarado-Mora, and João Rebello Pinho. Evolutionary rates and hbv: issues of rate estimation with bayesian molecular methods. *Antiviral therapy*, 2013.
- [4] Remco R. Bouckaert and Joseph Heled. Densitree 2: Seeing trees through the forest. *bioRxiv* <http://dx.doi.org/10.1101/012401>, 2014.
- [5] Remco R. Bouckaert, Joseph Heled, Denise Kühnert, Tim Vaughan, Chieh-Hsi Wu, Dong Xie, Marc A Suchard, Andrew Rambaut, and Alexei J Drummond. Beast 2: a software platform for bayesian evolutionary analysis. *PLoS Comput Biol*, 10(4):e1003537, Apr 2014.
- [6] Endymion D Cooper. Overly simplistic substitution models obscure green plant phylogeny. *Trends in plant science*, 19(9):576–582, 2014.
- [7] A. J. Drummond and M. A. Suchard. Bayesian random local clocks, or one rate to rule them all. *BMC biology*, 8(1):114, 2010.

- [8] Alexei J. Drummond and Remco R. Bouckaert. *Bayesian evolutionary analysis with BEAST*. Cambridge University Press, 2015.
- [9] Alexei J Drummond, Simon Y W Ho, Matthew J Phillips, and Andrew Rambaut. Relaxed phylogenetics and dating with confidence. *PLoS Biol*, 4(5):e88, May 2006.
- [10] Robert C Edgar. Muscle: multiple sequence alignment with high accuracy and high throughput. *Nucleic acids research*, 32(5):1792–1797, 2004.
- [11] J. Felsenstein. Evolutionary trees from dna sequences: a maximum likelihood approach. *Journal of Molecular Evolution*, 17:368–376, 1981.
- [12] Nicolas Galtier. Maximum-likelihood phylogenetic analysis under a covarion-like model. *Molecular Biology and Evolution*, 18(5):866–873, 2001.
- [13] Alexandra Gavryushkina, David Welch, Tanja Stadler, and Alexei J Drummond. Bayesian inference of sampled ancestor trees for epidemiology and fossil calibration. *PLoS computational biology*, 10(12):e1003919, 2014.
- [14] X Gu, Y X Fu, and W H Li. Maximum likelihood estimation of the heterogeneity of substitution rate among nucleotide sites. *Mol Biol Evol*, 12(4):546–57, Jul 1995.
- [15] Zhenhua Guo and John W Stiller. Comparative genomics and evolution of proteins associated with rna polymerase ii c-terminal domain. *Molecular biology and evolution*, 22(11):2166–2178, 2005.
- [16] Philippe H. and Lopez P. On the conservation of protein sequences in evolution. *Trends in biochemical sciences*, 26(7):414–416, 2001.
- [17] M. Hasegawa, H. Kishino, and T. Yano. Dating the human-ape splitting by a molecular clock of mitochondrial dna. *Journal of Molecular Evolution*, 22:160–174, 1985.
- [18] Wai Lok Sibon Li and Alexei J Drummond. Model averaging and bayes factor calculation of relaxed molecular clocks in bayesian phylogenetics. *Molecular biology and evolution*, 29(2):751–761, 2012.
- [19] Peter Lockhart, Phil Novis, Brook G Milligan, Jamie Riden, Andrew Rambaut, and Tony Larkum. Heterotachy and tree building: a case study with plastids and eubacteria. *Molecular biology and evolution*, 23(1):40–45, 2006.
- [20] Peter Lockhart and Mike Steel. A tale of two processes. *Systematic biology*, 54(6):948–951, 2005.
- [21] Peter J Lockhart, AW Larkum, M Steel, Peter J Waddell, and David Penny. Evolution of chlorophyll and bacteriochlorophyll: the problem of invariant sites in sequence analysis. *Proceedings of the National Academy of Sciences*, 93(5):1930–1934, 1996.

- [22] P Lopez, D Casane, and H Philippe. Heterotachy, an important process of protein evolution. *Molecular Biology and Evolution*, 19(1):1–7, 2002.
- [23] Mark Pagel and Andrew Meade. Modelling heterotachy in phylogenetic inference by reversible-jump markov chain monte carlo. *Philosophical Transactions of the Royal Society B: Biological Sciences*, 363(1512):3955–3964, 2008.
- [24] Hervé Philippe, Yan Zhou, Henner Brinkmann, Nicolas Rodrigue, and Frédéric Delsuc. Heterotachy and long-branch attraction in phylogenetics. *BMC evolutionary biology*, 5(1):50, 2005.
- [25] Bruce Rannala and Ziheng Yang. Inferring speciation times under an episodic molecular clock. *Systematic Biology*, 56(3):453–466, 2007.
- [26] MJ Sanderson, MJ Donoghue, WH Piel, and T Eriksson. Treebase: a prototype database of phylogenetic analyses and an interactive tool for browsing the phylogeny of life. *American Journal of Botany*, 81(6):183, 1994.
- [27] Harald Schneider, Eric Schuettpelz, Kathleen M Pryer, Raymond Cranfill, Susana Magallón, and Richard Lupia. Ferns diversified in the shadow of angiosperms. *Nature*, 428(6982):553–557, 2004.
- [28] Matthew Spencer, Edward Susko, and Andrew J Roger. Likelihood, parsimony, and heterogeneous evolution. *Molecular biology and evolution*, 22(5):1161–1164, 2005.
- [29] Edward Susko, Chris Field, Christian Blouin, and Andrew J Roger. Estimation of rates-across-sites distributions in phylogenetic substitution models. *Systematic biology*, 52(5):594–603, 2003.
- [30] Edward Susko, Yuji Inagaki, Chris Field, Michael E Holder, and Andrew J Roger. Testing for differences in rates-across-sites distributions in phylogenetic subtrees. *Molecular biology and evolution*, 19(9):1514–1523, 2002.
- [31] Koichiro Tamura, Joel Dudley, Masatoshi Nei, and Sudhir Kumar. Mega4: molecular evolutionary genetics analysis (mega) software version 4.0. *Molecular biology and evolution*, 24(8):1596–1599, 2007.
- [32] P. Waddell and D. Penny. Evolutionary trees of apes and humans from DNA sequences. In A. J. Lock and C. R. Peters, editors, *Handbook of symbolic evolution*, pages 53–73. Clarendon Press, Oxford., 1996.
- [33] Simon Whelan, Benjamin P Blackburne, and Matthew Spencer. Phylogenetic substitution models for detecting heterotachy during plastid evolution. *Molecular biology and evolution*, 28(1):449–458, 2011.
- [34] Ziheng Yang. Maximum likelihood phylogenetic estimation from DNA sequences with variable rates over sites: Approximate methods. *Journal of Molecular Evolution*, 39(3):306–314, 1994.

- [35] G.U. Yule. A mathematical theory of evolution based on the conclusions of dr. j.c. willis. *Philosophical Transactions of the Royal Society of London, Series B*, 213:21–87, 1924.

## Appendix A: List of alignments from TreeBase

Alignment numbers from <http://treebase.org>

Matrix ID	# taxa	# sites	Description sourced from TreeBase
M229	29	634	Tomentellopsis ITS
M247	12	859	Anamika ITS
M248	22	1573	Anamika LSU
M835	31	859	Descoea clade
M1285	25	2088	Osedax
M1460	49	981	GHR
M1499	12	1681	Chromosome Y
M1526	43	1866	Byeeye gapsmissing
M1560	19	348	Celastrales ITS1
M1563	11	1930	Auritella-11
M1711	46	6431	Simultaneous-Aniso
M1842	23	1986	Lymania cpDNA& (growth hormone receptor)
M1976	4	1486	Fig. 2
M1998	38	2124	trnLF ITS ETS Abrahamia
M2681	40	606	atp6 all fungi
M3420	6	1863	Fig2A 18SrDNA
M3483	33	605	Ceratobasidium
M3717	24	1921	Anolis Lizards
M3797	41	2395	trnL-F
M4370	50	908	ITS
M4557	32	732	32 OTUs ITS
M4642	39	1078	Ceratium 39x1078
M5884	42	2198	Malvaceae s.l.
M6327	48	860	Stromatonectria LSU
M7295	16	2113	Thamnosma
M8090	17	938	vWF11
M10235	21	1153	Cuscuta chinensis matrix
M10430	8	488	Cystotheca tjibodensis & Abcb9-intron-2
M10797	45	612	Euphorbiaceae ITS1 ITS2
M11101	34	6388	nuclear and mit genes
M11666	35	1909	Locus 81
M12139	14	9076	Drosophila virilis 16s adh fu gpdh nonA CG9631 CG7219 alignment
M12273	28	3646	Ingroup MIT all x28
M12814	27	539	ITS Character Matrix
M13381	7	1727	Catathelasma
M13946	36	881	Postia s.l. LSU
M14113	17	1175	Pseudofusicoccum
M15777	15	858	Matrix Rickettsia
M16364	5	3612	bik1 matrix
M16929	13	8473	Anura no missing & sp ITS AG-A
M17631	10	585	Fibrodontia alba sp. nov. ITS
M18066	15	535	ErythromadaMB & + rpl16 matrix 2395x41
M18080	9	555	PhysalosporaMB
M19483	30	2770	Oryza sativa Waxy gene nexus format
M19789	15	280	Mammal
M21273	20	1590	Spirochaeta
M23904	18	1330	Sticherus rbcL
M24214	14	587	Cephalopholis & ITS matK rbcL-atpB sp.
M24498	13	1521	Streptomyces sannanensis strain SU118
M25014	14	3363	Myxobasis



Summary table for nucleotide sequences from TreeBase. The number in first column coincides with numbers in Figure 3

	Dataset	4gi			4mgi			4rgi		
		logL	AICM	Height	logL	AICM	Height	logL	AICM	Height
1	M19789	-2136.8475	4308.693	0.3928786266	-2132.9903	4316.91	0.4022	-2135.3667	4315.194	0.3495
2	M10430	-1204.2801	2425.789	0.1307	-1202.565	2422.413	0.1239	-1204.3171	2424.995	0.1361
3	M18080	-1950.8533	3919.156	0.1597	-1949.9263	3924.941	0.1663	-1950.7097	3921.987	0.1472
4	M17631	-3460.2928	6941.796	0.7876	-3451.878	6931.547	0.7186	-3454.9799	6945.568	0.7819
5	M1976	-3540.447	7088.348	0.1163	-3537.0736	7087.692	0.1079	-3539.7286	7093.989	0.1145
6	M1560	-3136.5259	6312.933	0.4957	-3138.8655	6335.85	0.4928	-3136.0007	6309.815	0.4847
7	M18066	-2675.0575	5385.319	0.1589	-2665.2159	5380.643	0.1572	-2667.068	5399.271	0.1621
8	M24214	-907.8032	1839.586	0.0043297	-907.8311	1838.779	0.0044378	-907.7367	1838.841	0.0045036
9	M247	-2933.511	5914.866	0.1612	-2927.1371	5903.733	0.154	-2928.0852	5913.916	0.1538
10	M3420	-3118.0111	6246.542	0.0225	-3117.3701	6247.134	0.0232	-3117.6888	6247.359	0.0227
11	M15777	-1824.6666	3685.85	0.0271	-1822.5692	3678.614	0.0243	-1824.8101	3691.549	0.028
12	M13381	-3714.5649	7452.41	0.0481	-3714.1537	7454.202	0.0463	-3714.6251	7451.283	0.0471
13	M12814	-937.2828	1911.745	0.0071562	-936.8968	1908.188	0.0068783	-937.2707	1911.323	0.0068832
14	M8090	-2738.5756	5508.114	0.0497	-2736.4928	5506.812	0.0492	-2738.9789	5504.87	0.0495
15	M229	-2187.3138	4429.037	0.0678	-2186.4342	4435.671	0.0687	-2188.3429	4434.021	0.0692
16	M14113	-2898.4699	5823.49	0.4174	-2897.5843	5822.312	0.6306	-2897.8555	5824.87	0.6475
17	M3483	-1975.2533	4012.721	0.0372	-1971.3285	4012.63	0.0363	-1974.4593	4025.041	0.0359
18	M24498	-2755.5961	5556.459	0.0176	-2751.7179	5560.086	0.0201	-2753.6969	5561.925	0.0186
19	M1499	-3125.8316	6273.332	0.0246	-3125.6009	6273.723	0.0242	-3125.2416	6272.231	0.0239
20	M16364	-13356.1059	26724.697	1.1466	-13348.8267	26717.337	3.3584	-13353.093	26725.96	1.1155
21	M1563	-5890.6771	11810.842	0.1149	-5886.5602	11810.292	0.1235	-5890.5648	11815.067	0.1149
22	M23904	-3275.5349	6581.852	0.0439	-3273.1268	6583.667	0.0447	-3275.3788	6586.233	0.0436
23	M10235	-2703.819	5450.485	0.0289	-2703.3143	5453.441	0.0315	-2704.2486	5465.889	0.0324
24	M4557	-2971.1893	6014.962	0.0907	-2964.7763	6029.154	0.0916	-2970.2121	6015.927	0.0875
25	M2681	-9846.1911	19803.672	0.9047	-9727.154	19606.03	0.6464	-9731.0339	19680.873	0.6493
26	M835	-4292.5875	8663.089	0.1482	-4280.587	8660.828	0.1579	-4283.0637	8685.92	0.1585
27	M10797	-8018.9627	16144.199	0.475	-7993.7406	16157.387	0.4966	-8016.2651	16170.728	0.4762
28	M13946	-4078.8918	8226.82	0.0736	-4061.1762	8220.067	0.0735	-4065.0459	8267.309	0.0754
29	M21273	-9533.7946	19111.588	0.2792	-9490.9268	19048.554	0.2012	-9495.1618	19073.77	0.4941
30	M248	-4210.2705	8482.219	0.075	-4185.5152	8457.427	0.0626	-4183.9474	8487.001	0.0753
31	M7295	-4694.4796	9413.209	0.0526	-4691.2445	9412.467	0.0552	-4693.9381	9416.621	0.0536
32	M6327	-4813.2593	9774.09	0.0723	-4776.1245	9731.539	0.0653	-4784.6078	9827.737	0.0738
33	M4642	-2707.7318	5481.546	0.0227	-2703.4576	5489.916	0.0209	-2705.4797	5498.721	0.0191
34	M1842	-3110.2733	6270.127	0.0070593	-3109.9808	6273.357	0.0070998	-3110.0356	6266.374	0.0070534
35	M3717	-21781.2882	43634.435	0.5391	-21763.6884	43629.967	0.5323	-21770.0847	43616.439	0.5159
36	M4370	-4529.6939	9159.546	0.1538	-4511.5996	9141.707	0.1788	-4515.0267	9184.345	0.17
37	M1460	-6946.0161	14019.666	0.0792	-6928.8923	14030.192	0.0786	-6940.5631	14057.9	0.0784
38	M25014	-7314.2152	14662.746	0.0453	-7302.0321	14656.572	0.0472	-7305.4891	14675.943	0.0453
39	M1285	-13355.6276	26766.856	0.3152	-13271.5138	26650.638	0.2716	-13274.5577	26664.298	0.2751
40	M11666	-2911.0707	5853.877	0.0017217	-2910.846	5854.405	0.0018171	-2911.5679	5858.014	0.0016958
41	M1526	-5664.4201	11453.866	0.024	-5631.2512	11441.508	0.0249	-5626.6066	11439.015	0.025
42	M1998	-11564.6916	23200.15	0.1683	-11515.8625	23163.982	0.1239	-11518.8415	23192.211	0.0984
43	M19483	-4708.4409	9486.533	0.0113	-4698.736	9460.552	0.0126	-4693.856	9460.117	0.0109
44	M5884	-6898.4465	13882.141	0.0277	-6882.9889	13879.288	0.0293	-6880.2777	13906.713	0.0268
45	M3797	-5973.4118	12052.914	0.0208	-5965.0801	12045.769	0.0169	-5968.6401	12046.771	0.0179
46	M12273	-22793.8586	45669.023	0.1936	-22705.5187	45530.638	0.2818	-22711.8045	45561.898	0.2701
47	M16929	-29828.8968	59687.073	0.0706	-29782.9779	59619.427	0.1097	-29785.2618	59640.032	0.0789
48	M12139	-29070.5222	58173.63	0.1259	-29035.189	58123.616	0.1082	-29035.8247	58119.319	0.109
49	M11101	-47426.5181	94952.268	0.3398	-47299.4892	94768.779	0.2003	-47301.207	94755.571	0.1572
50	M1711	-38627.0072	77368.97	0.1044	-38543.7533	77260.275	0.0957	-38547.8281	77260.311	0.1038

## Appendix B: Genbank sequences

Name	Genbank accession number
<i>Arabidopsis thaliana</i>	NC_000932
<i>Acorus calamus</i>	NC_007407
<i>Amborella trichopoda</i>	NC_005086
<i>Cryptomeria japonica</i>	NC_010548
<i>Taiwania cryptomerioides</i>	NC_016065
<i>Cycas taitungensis</i>	NC_009618
<i>Welwitschia mirabilis</i>	NC_010654
<i>Ephedra equisetina</i>	NC_011954
<i>Anthoceros formosae</i>	NC_004543
<i>Syntrichia ruralis</i>	NC_012052
<i>Chara vulgaris</i>	NC_008097
<i>Chlorokybus atmophyticus</i>	NC_008822
<i>Chaetosphaeridium globosum</i>	NC_004115
<i>Huperzia lucidula</i>	NC_006861
<i>Isoetes flaccida</i>	NC_014675
<i>Selaginella moellendorffii</i>	NC_013086
<i>Selaginella uncinata</i>	AB197035
<i>Aneura mirabilis</i>	NC_010359
<i>Marchantia polymorpha</i>	NC_001319
<i>Ptilidium pulcherrimum</i>	NC_015402
<i>Mesostigma viride</i>	NC_002186
<i>Adiantum capillus-veneris</i>	NC_004766
<i>Alsophila spinulosa</i>	NC_012818
<i>Angiopteris evecta</i>	NC_008829
<i>Cheilanthes lindheimeri</i>	NC_014592
<i>Equisetum arvense</i>	NC_014699
<i>Psilotum nudum</i>	NC_003386
<i>Pteridium aquilinum</i>	NC_014348
<i>Staurostrum punctulatum</i>	NC_008116
<i>Zygnema circumcarinatum</i>	NC_008117
<i>Chlorella variabilis</i>	NC_015359
<i>Oocystis solitaria</i>	FJ968739
<i>Parachlorella kessleri</i>	NC_012978
<i>Pedinomonas minor</i>	NC_016733
<i>Leptosira terrestris</i>	NC_009681

## Appendix C: XML for green plants and algae analysis

All BEAST XML files can be downloaded from here: <https://www.cs.auckland.ac.nz/~remco/MGSMxml.tgz>.

All analyses uses partitions for each 3 codon positions, a reversible-jump based substitution model, uncorrelated log normal clock model and Yule tree prior.

atpB = atpB chloroplast gene from green plants and algae

rpoc = rpoC1 chloroplast gene from green plants and algae

atprpo = atpB and rpoC1 genes concatenated

atpB.RB4g.ucln.yule.xml	single gamma site categories, one gamma per partition
atpB.RB4spm.g.ucln.yule.xml	multi gamma site model, one gamma per branch (shared among partitions)
atpB.RB8spm.g.ucln.yule.xml	"
atpB.RB4mg.ucln.yule.xml	multi gamma site model, one gamma per partition per branch
atpB.RB8mg.ucln.yule.xml	"
atpB.RB4gi.ucln.yule.xml	single gamma site categories, one gamma per partition + invariant sites
atpB.RB4mgi.ucln.yule.xml	multi gamma site model, one gamma per branch per partition + invariant sites
atpB.RB4rmgi.ucln.yule.xml	relaxed gamma site model, one gamma per branch + invariant sites
atpB.RB43rmgi.ucln.yule.xml	relaxed gamma site model, one gamma per branch per partition + invariant sites
rpoc.RB4g.ucln.yule.xml	single gamma site categories, one gamma per partition
rpoc.RB4spm.g.ucln.yule.xml	multi gamma site model, one gamma per branch (shared among partitions)
rpoc.RB8spm.g.ucln.yule.xml	"
rpoc.RB4mg.ucln.yule.xml	multi gamma site model, one gamma per partition per branch
rpoc.RB8mg.ucln.yule.xml	"
rpoc.RB4gi.ucln.yule.xml	single gamma site categories, one gamma per partition + invariant sites
rpoc.RB4mgi.ucln.yule.xml	multi gamma site model, one gamma per branch per partition + invariant sites
rpoc.RB4rmgi.ucln.yule.xml	relaxed gamma site model, one gamma per branch + invariant sites
rpoc.RB43rmgi.ucln.yule.xml	relaxed gamma site model, one gamma per branch per partition + invariant sites
atprpo.RB4gi.ucln.yule.xml	single gamma site categories, one gamma per partition + invariant sites
atprpo.RB4mgi.ucln.yule.xml	multi gamma site model, one gamma per branch per partition + invariant sites

## Appendix D: Results for partition finder repository data

Comparing single and multi-gamma site models.

	Delta logL	Delta AICM	Height	min(ESS)
Bergsten2013	60.3459	-104.168	-18.4345281639	233.9029
Caterino2001	54.834	-26.444	10.6810387065	103.5102
Delsuc2003	25.1585	-33.03	-2.9676258993	249.2825
Dsouli2011	58.7006	-60.973	-8.1706435286	120.4567
Endicott2008	42.0513	-14.217	1.7730404264	107.0668
Fishbein2001	79.6407	-81.564	5.3448275862	102.6875
Kang2013b	24.7453	-23.423	-8.867427568	133.3271
Sauquet2011	60.853	-83.947	-6.3829787234	97.4762

Other datasets did not get to convergence.